NATIONAL ADVISORY COMMITTEE FOR AERONAUTICS

REPORT No. 614

PRESSURE DISTRIBUTION OVER AN N. A. C. A. 23012 AIRFOIL WITH AN N. A. C. A. 23012 EXTERNAL-AIRFOIL FLAP

By CARL J. WENZINGER

1938

For sale by the Superintendent of Documents, Washington, D. C. - - - - - - - - - - - - - Price 10 cents
Subscription price, $3.00 per year

AERONAUTIC SYMBOLS

1. FUNDAMENTAL AND DERIVED UNITS

	Symbol	Metric		English	
		Unit	Abbreviation	Unit	Abbreviation
Length	l	meter	m	foot (or mile)	ft. (or mi.)
Time	t	second	s	second (or hour)	sec. (or hr.)
Force	F	weight of 1 kilogram	kg	weight of 1 pound	lb.
Power	P	horsepower (metric)		horsepower	hp.
Speed	V	kilometers per hour	k.p.h.	miles per hour	m.p.h.
		meters per second	m.p.s.	feet per second	f.p.s.

2. GENERAL SYMBOLS

W, Weight $=mg$

g, Standard acceleration of gravity $=9.80665$ m/s^2 or 32.1740 ft./sec.^{2}

m, Mass $=\frac{W}{g}$

I, Moment of inertia $=mk^2$. (Indicate axis of radius of gyration k by proper subscript.)

μ, Coefficient of viscosity

ν, Kinematic viscosity

ρ, Density (mass per unit volume)

Standard density of dry air, 0.12497 kg-m^{-4}-s^2 at 15° C. and 760 mm; or 0.002378 lb.-ft.$^{-4}$ sec.^{2}

Specific weight of "standard" air, 1.2255 kg/m^3 or 0.07651 lb./cu. ft.

3. AERODYNAMIC SYMBOLS

S, Area

S_w, Area of wing

G, Gap

b, Span

c, Chord

$\frac{b^2}{S}$, Aspect ratio

V, True air speed

q, Dynamic pressure $=\frac{1}{2}\rho V^2$

L, Lift, absolute coefficient $C_L=\frac{L}{qS}$

D, Drag, absolute coefficient $C_D=\frac{D}{qS}$

D_0, Profile drag, absolute coefficient $C_{D_0}=\frac{D_0}{qS}$

D_i, Induced drag, absolute coefficient $C_{D_i}=\frac{D_i}{qS}$

D_p, Parasite drag, absolute coefficient $C_{D_p}=\frac{D_p}{qS}$

C, Cross-wind force, absolute coefficient $C_C=\frac{C}{qS}$

R, Resultant force

i_w, Angle of setting of wings (relative to thrust line)

i_t, Angle of stabilizer setting (relative to thrust line)

Q, Resultant moment

Ω, Resultant angular velocity

$\rho\frac{Vl}{\mu}$, Reynolds Number, where l is a linear dimension (e.g., for a model airfoil 3 in. chord, 100 m.p.h. normal pressure at 15° C., the corresponding number is 234,000; or for a model of 10 cm chord, 40 m.p.s., the corresponding number is 274,000)

C_p, Center-of-pressure coefficient (ratio of distance of c.p. from leading edge to chord length)

α, Angle of attack

ϵ, Angle of downwash

α_0, Angle of attack, infinite aspect ratio

α_i, Angle of attack, induced

α_a, Angle of attack, absolute (measured from zero-lift position)

γ, Flight-path angle

REPORT No. 614

PRESSURE DISTRIBUTION OVER AN N. A. C. A. 23012 AIRFOIL WITH AN N. A. C. A. 23012 EXTERNAL-AIRFOIL FLAP

By CARL J. WENZINGER

Langley Memorial Aeronautical Laboratory

22915—37——1

NATIONAL ADVISORY COMMITTEE FOR AERONAUTICS

HEADQUARTERS, NAVY BUILDING, WASHINGTON, D. C.

LABORATORIES, LANGLEY FIELD, VA.

Created by act of Congress approved March 3, 1915, for the supervision and direction of the scientific study of the problems of flight (U. S. Code, Title 50, Sec. 151). Its membership was increased to 15 by act approved March 2, 1929. The members are appointed by the President, and serve as such without compensation.

TECHNICAL COMMITTEES

AERODYNAMICS
POWER PLANTS FOR AIRCRAFT
AIRCRAFT MATERIALS
AIRCRAFT STRUCTURES
AIRCRAFT ACCIDENTS
INVENTIONS AND DESIGNS

Coordination of Research Needs of Military and Civil Aviation

Preparation of Research Programs

Allocation of Problems

Prevention of Duplication

Consideration of Inventions

LANGLEY MEMORIAL AERONAUTICAL LABORATORY

LANGLEY FIELD, VA.

Unified conduct, for all agencies, of scientific research on the fundamental problems of flight.

OFFICE OF AERONAUTICAL INTELLIGENCE

WASHINGTON, D. C.

Collection, classification, compilation, and dissemination of scientific and technical information on aeronautics.

REPORT No. 614

PRESSURE DISTRIBUTION OVER AN N. A. C. A. 23012 AIRFOIL WITH AN N. A. C. A. 23012 EXTERNAL-AIRFOIL FLAP

By CARL J. WENZINGER

SUMMARY

Pressure-distribution tests of an N. A. C. A. 23012 airfoil with an N. A. C. A. 23012 external-airfoil flap were made in the 7- by 10-foot wind tunnel. The pressures were measured on the upper and lower surfaces at one chord section on both the main airfoil and on the flap for several different flap deflections and at several angles of attack. A test installation was used in which the airfoil was mounted horizontally in the wind tunnel between vertical end planes so that two-dimensional flow was approximated.

The data are presented in the form of pressure-distribution diagrams and as graphs of calculated coefficients for the airfoil-and-flap combination and for the flap alone. The pressure-distribution tests showed that, as with other types of flap, the greater part of the increment of total maximum lift due to deflecting the external-airfoil flap downward arises from the increased load carried by the main airfoil. The maximum normal-force coefficient of the external-airfoil flap was about the same as that of a split flap. The hinge moments, however, were much lower because of the axis location used with the external-airfoil flap. The pressure diagrams showed that, when the plain airfoil and the flapped airfoil are compared at the same total lift, the flap reduces the adverse pressure gradients and the tendency of the main airfoil to stall. When the plain and flapped airfoils are compared at the same angle of attack, it is apparent that the flap influences the air flow around the main airfoil so that the airfoil carries a much greater load without stalling than is possible without the flap.

INTRODUCTION

The external-airfoil flap in combination with a main airfoil appears to be one of the most generally satisfactory high-lift devices investigated up to the present time. Previous investigations of this arrangement (references 1, 2, and 3) have shown that it is capable of developing high lift coefficients and that it gives lower drag at these high lift coefficients than do plain or split flaps.

Several different combinations of airfoil section for both the main airfoil and the flap have been investigated; the most promising arrangement thus far obtained has the N. A. C. A. 23012 section for both main airfoil and flap. In addition, a survey of the flap hinge-axis location has been made (reference 2) to obtain one that would give low flap-operating moments and good aerodynamic characteristics.

In order to complete the information required for structural-design purposes, pressure-distribution tests were made to obtain the air-load distribution over the main airfoil and flap. The combination tested has the N. A. C. A. 23012 section for both main airfoil and flap and uses the hinge axis previously developed for this flap.

APPARATUS AND TESTS

MODEL

The main airfoil was built of laminated mahogany to the N. A. C. A. 23012 profile and has a span and chord each of 20 inches. The external-airfoil flap was built of brass, also to the N. A. C. A. 23012 profile, and has a span of 20 inches and a chord of 4 inches (20 percent of the main airfoil chord). The flap was supported on the main airfoil by metal fittings at each end and by two intermediate fittings spaced equally along the span. The flap hinge axis (see fig. 1) was that previously developed as described in reference 2, the flap being arranged for locking at any desired deflection between $-10°$ and $60°$.

A main row of pressure orifices was built into the upper and lower surfaces of both the main airfoil and the external-airfoil flap at the midspan section. These orifices were located on the model as tabulated in figure 1, the tubes from the orifices being brought through the model and out at one end. The pressures were photographically recorded by a multiple-tube manometer.

Two auxiliary rows of pressure orifices were also built into the upper and lower surfaces of only the main airfoil, one row being located 2 inches and the other row ½ inch from the end. These orifices, together with those at the midspan location, were used incidentally to measure the distribution of pressures along the span of the model between end planes for a few conditions.

TEST INSTALLATION

The model was mounted in the N. A. C. A. 7- by 10-foot open-jet wind tunnel (reference 4) as shown by figure 2. The main airfoil was rigidly attached to two large circular end plates to which the flap was also fastened but arranged to rotate so that its setting might be changed. The two end plates were supported in

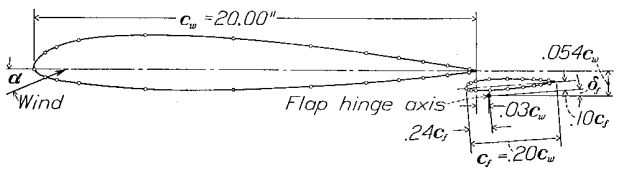

FIGURE 1.—Cross section of model showing orifice locations used in pressure-distribution tests. N. A. C. A. 23012 airfoil with 0.20c_w 23012 external-airfoil flap.

Orifice	Location from leading edge—	
	Of wing (fractions c_w)	Of flap (fractions c_f)
0	0.000	0.000
1	.024	.025
2	.050	.050
3	.100	.100
4	.250	.250
5	.450	.450
6	.625	.625
7	.750	.750
8	.825	.825
9	.881	.925
10	.936	----------
11	.986	----------

circular cut-outs in two large vertical end planes that extended from top to bottom of the air stream and some distance ahead of and behind the model. The angle of attack of the model was set by rotating the large circular plates and locking them at the desired angle. Approximately two-dimensional flow is obtained with this type of installation and the section characteristics of the model under test may be determined.

TESTS

The tests were all carried out at a dynamic pressure of 16.37 pounds per square foot, corresponding to an air speed of 80 miles per hour at standard sea-level conditions. The average test Reynolds Number, based on the sum of the main airfoil and flap chords, was 1,460,000. This test Reynolds Number, when converted to an effective Reynolds Number (reference 5) that takes account of the turbulence in the air stream, is 2,040,000. (Effective Reynolds Number = test Reynolds Number × turbulence factor; turbulence factor for the tunnel is 1.4.)

The model was tested with the external-airfoil flap set at angles of −3°, 0°, 10°, 20°, 30°, and 40°. The main airfoil was also tested by itself without the flap for purposes of comparison. The angles of attack ranged from −16° to 16° and the lift coefficients included those from approximately maximum negative to maximum positive. With the model at a given angle of attack and with a given flap setting, a few minutes were allowed for all test conditions to become steady; a record was then taken of the pressures at the orifices by means of the photographic manometer.

PRESENTATION OF DATA

PRESSURE DIAGRAMS

Diagrams of the pressures over the upper and lower surfaces of the main airfoil without flap (fig. 3) are given as ratios of orifice pressure p to dynamic pressure of the air stream q for the angles of attack investigated.

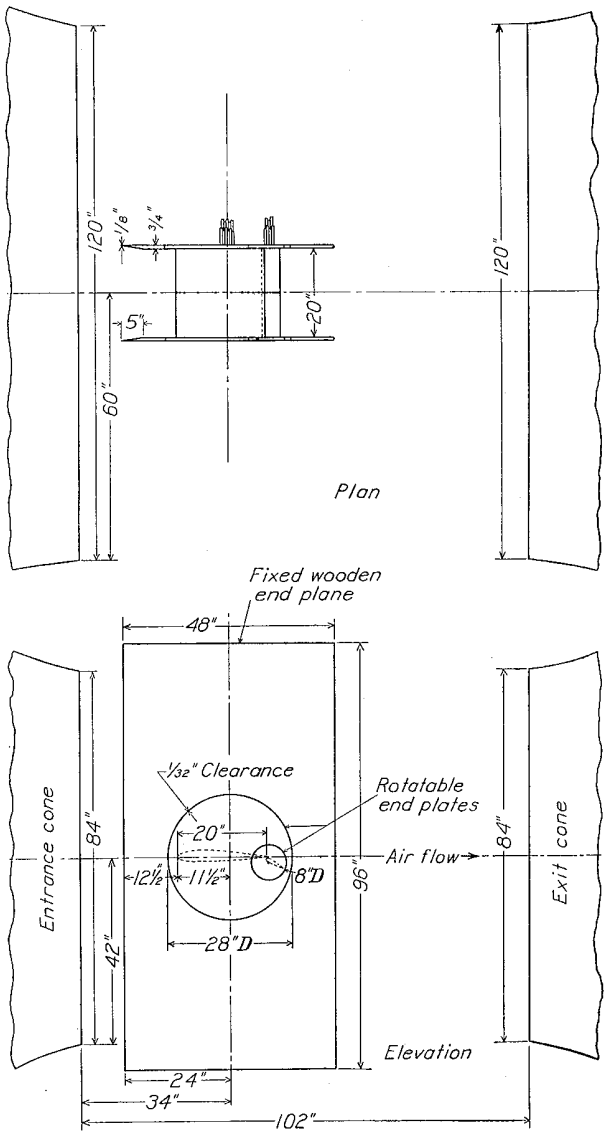

FIGURE 2.—Diagram of model with external-airfoil flap installed between end planes in the 7- by 10-foot wind tunnel.

Pressure diagrams for the combination of main airfoil with external-airfoil flap are given in figures 4 to 11 for the various flap deflections and angles of attack tested. On the diagrams the pressures are plotted normal to the main-airfoil chord and to the flap chord, the pressure values being measured from the main chord for the main-airfoil pressures and from the flap chord for the flap pressures.

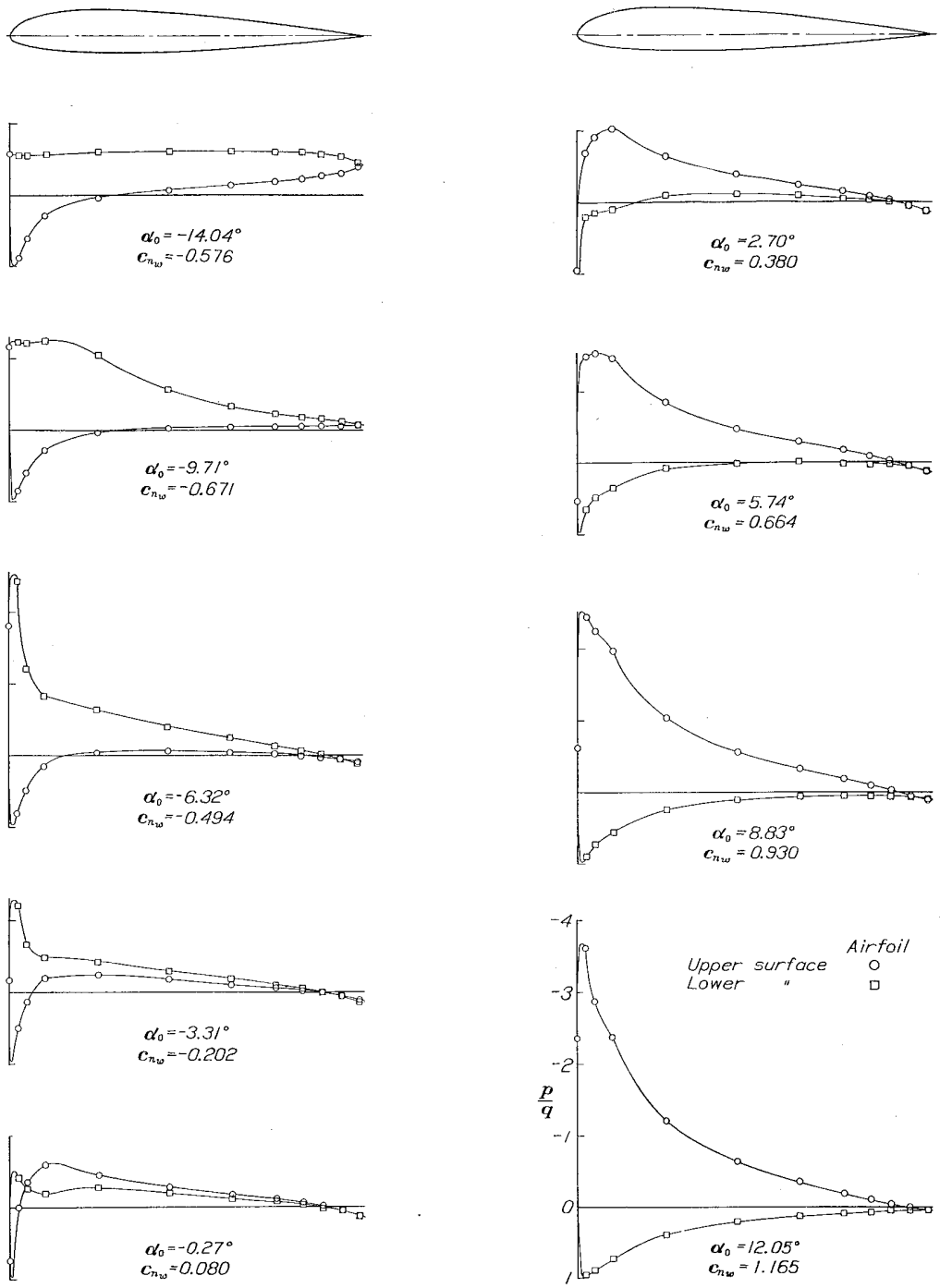

FIGURE 3.—Pressure distribution on the N. A. C. A. 23012 main airfoil without flaps at various angles of attack.

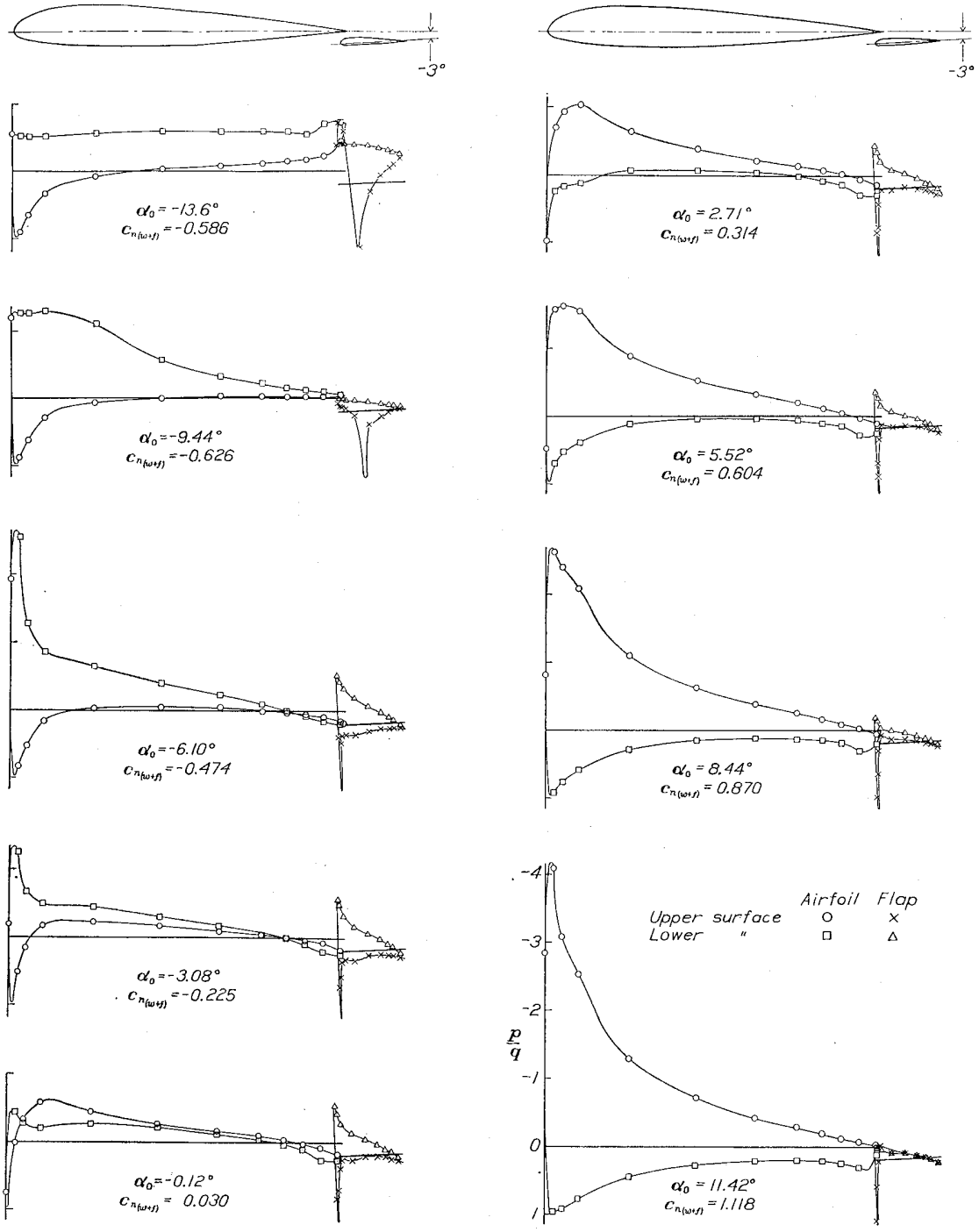

FIGURE 4.—Pressure distribution on the N. A. C. A. 23012 airfoil with N. A. C. A. 23012 external-airfoil flap at various angles of attack. Flap deflected −3°.

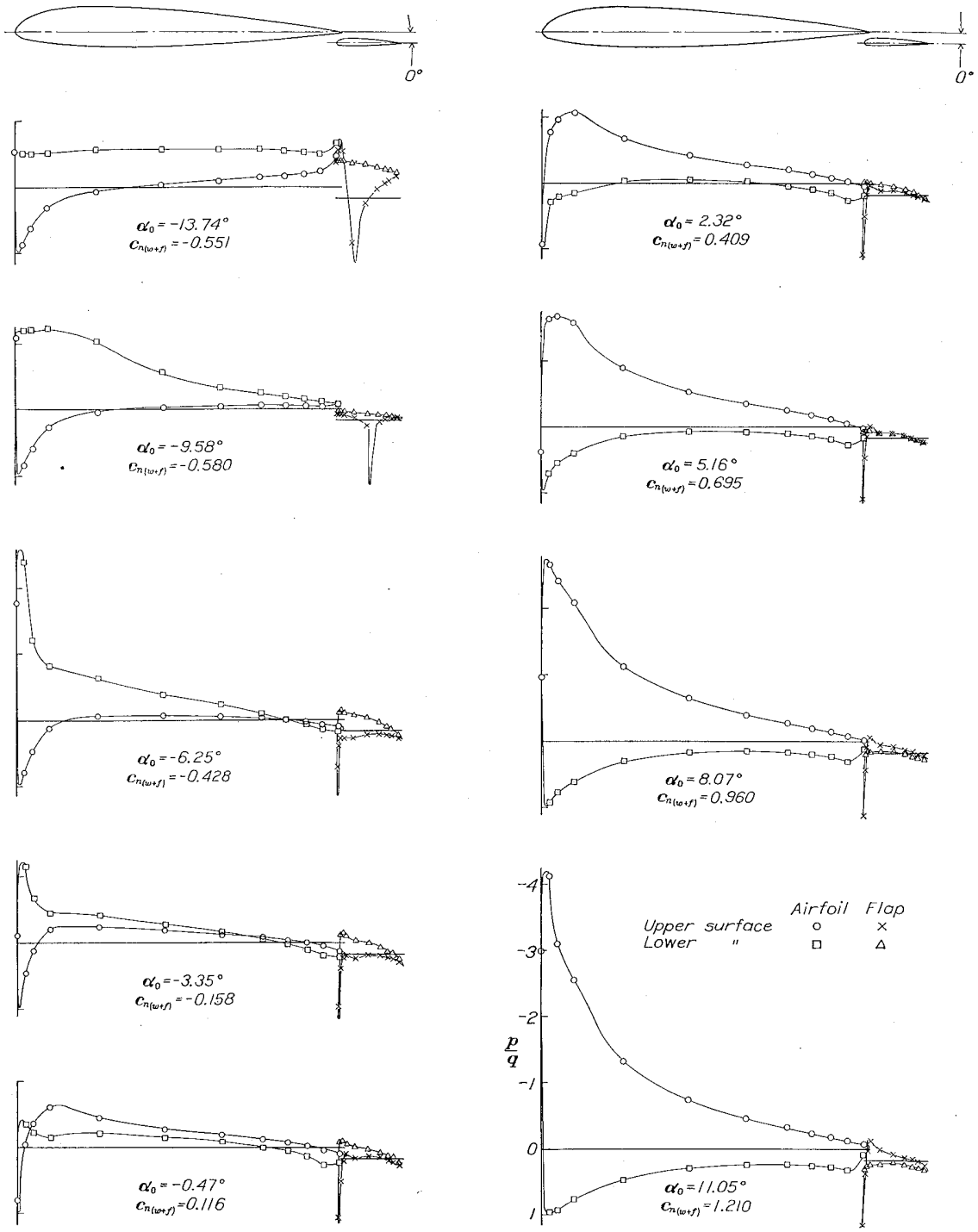

FIGURE 5.—Pressure distribution on the N. A. C. A. 23012 airfoil with N. A. C. A. 23012 external-airfoil flap at various angles of attack. Flap deflected 0°.

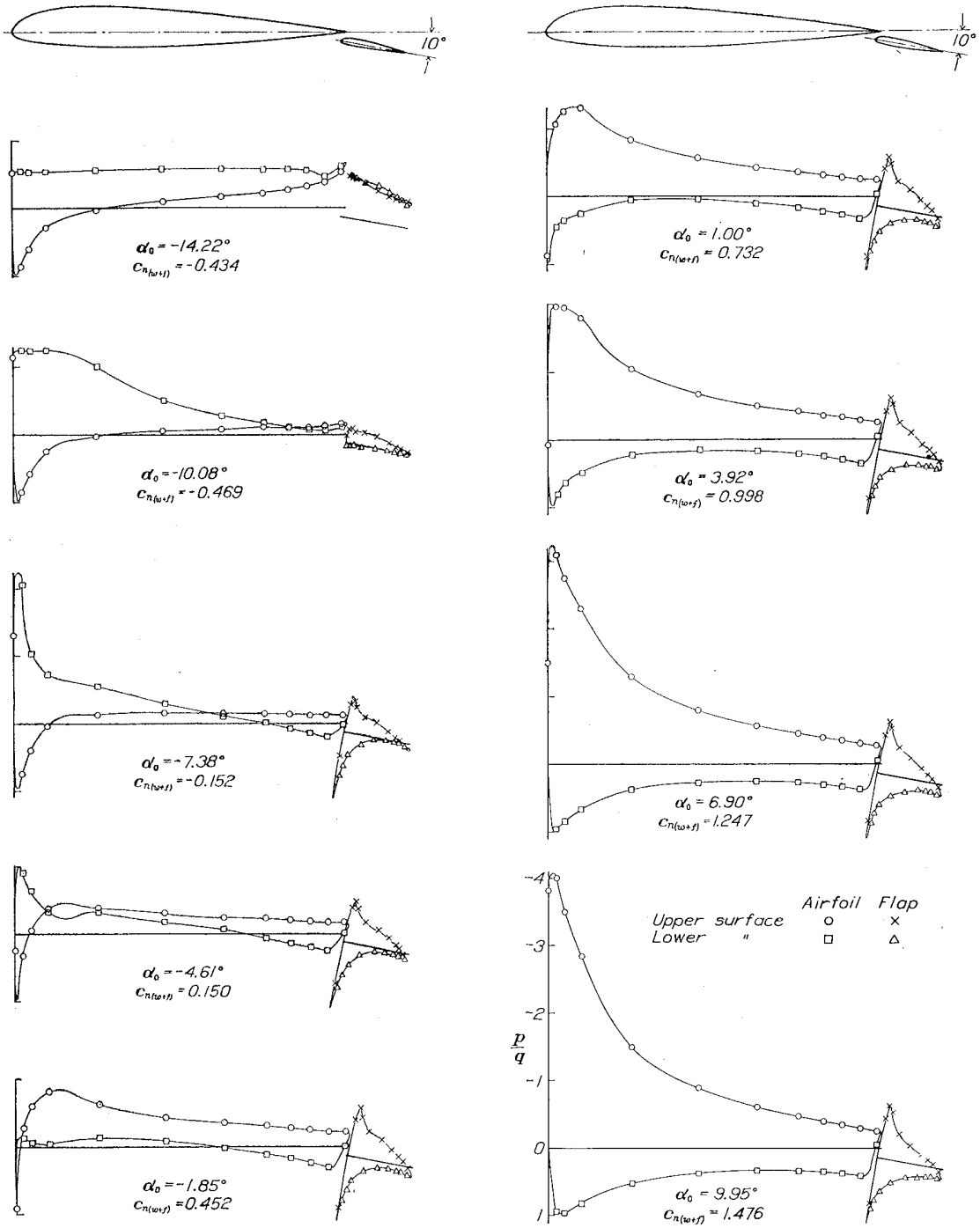

FIGURE 6.—Pressure distribution on the N. A. C. A. 23012 airfoil with N. A. C. A. 23012 external-airfoil flap at various angles of attack. Flap deflected 10°.

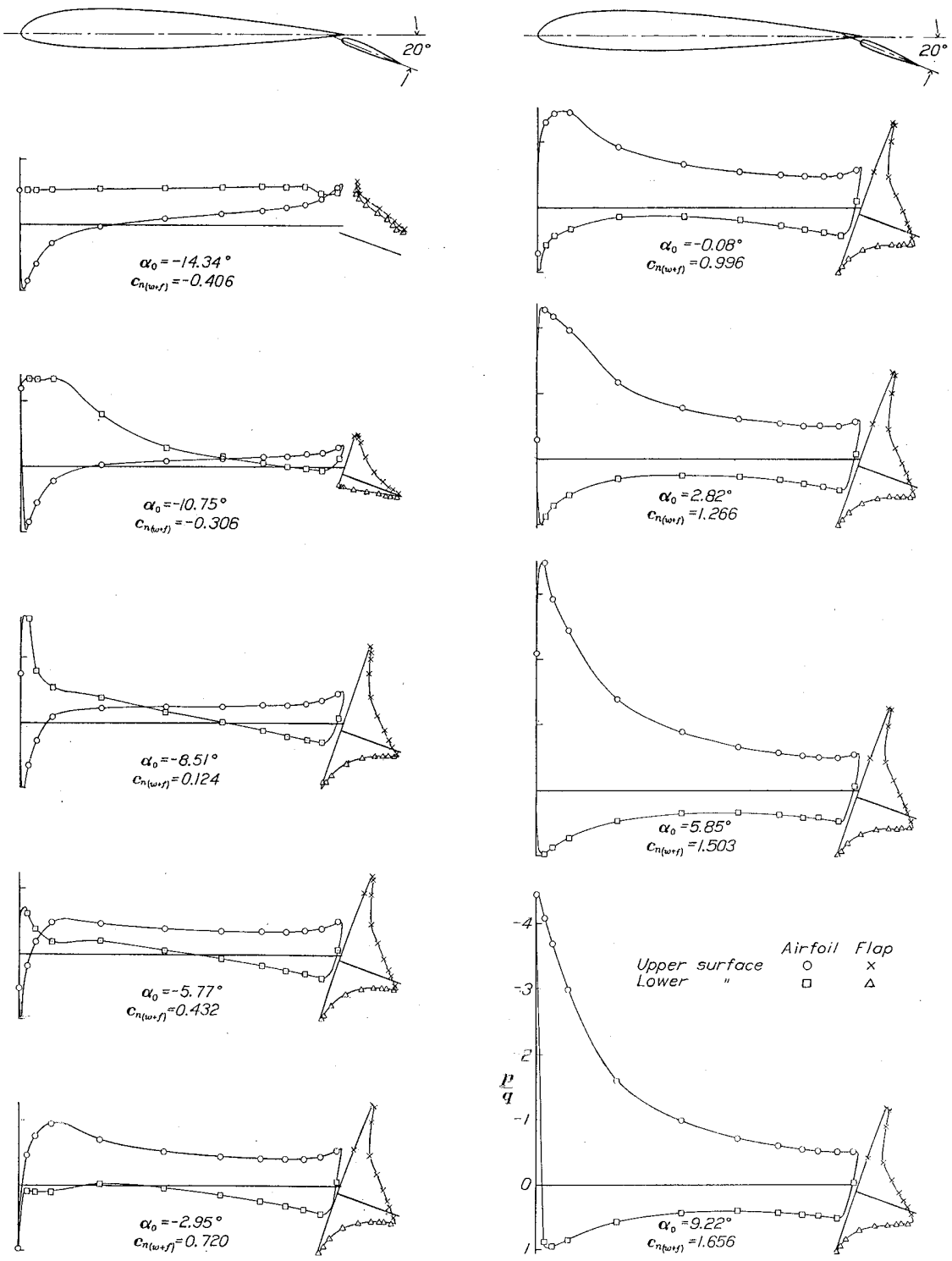

FIGURE 7.—Pressure distribution on the C. N. A. A. 23012 airfoil with N. A. C. A. 23012 external-airfoil flap at various angles of attack. Flap deflected 20°.

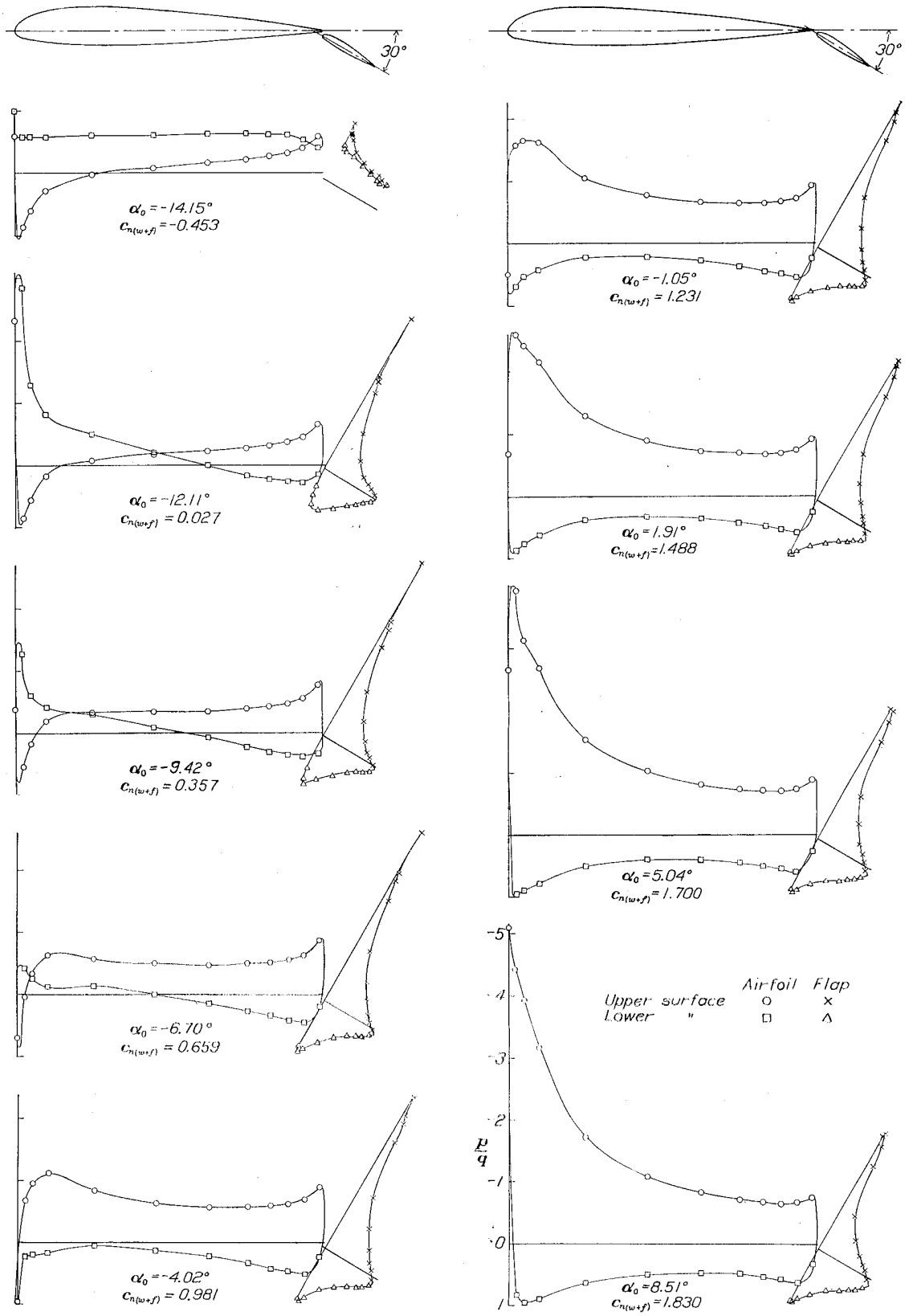

FIGURE 8.—Pressure distribution on the N. A. C. A. 23012 airfoil with N. A. C. A. 23012 external-airfoil flap at various angles of attack. Flap deflected 30°.

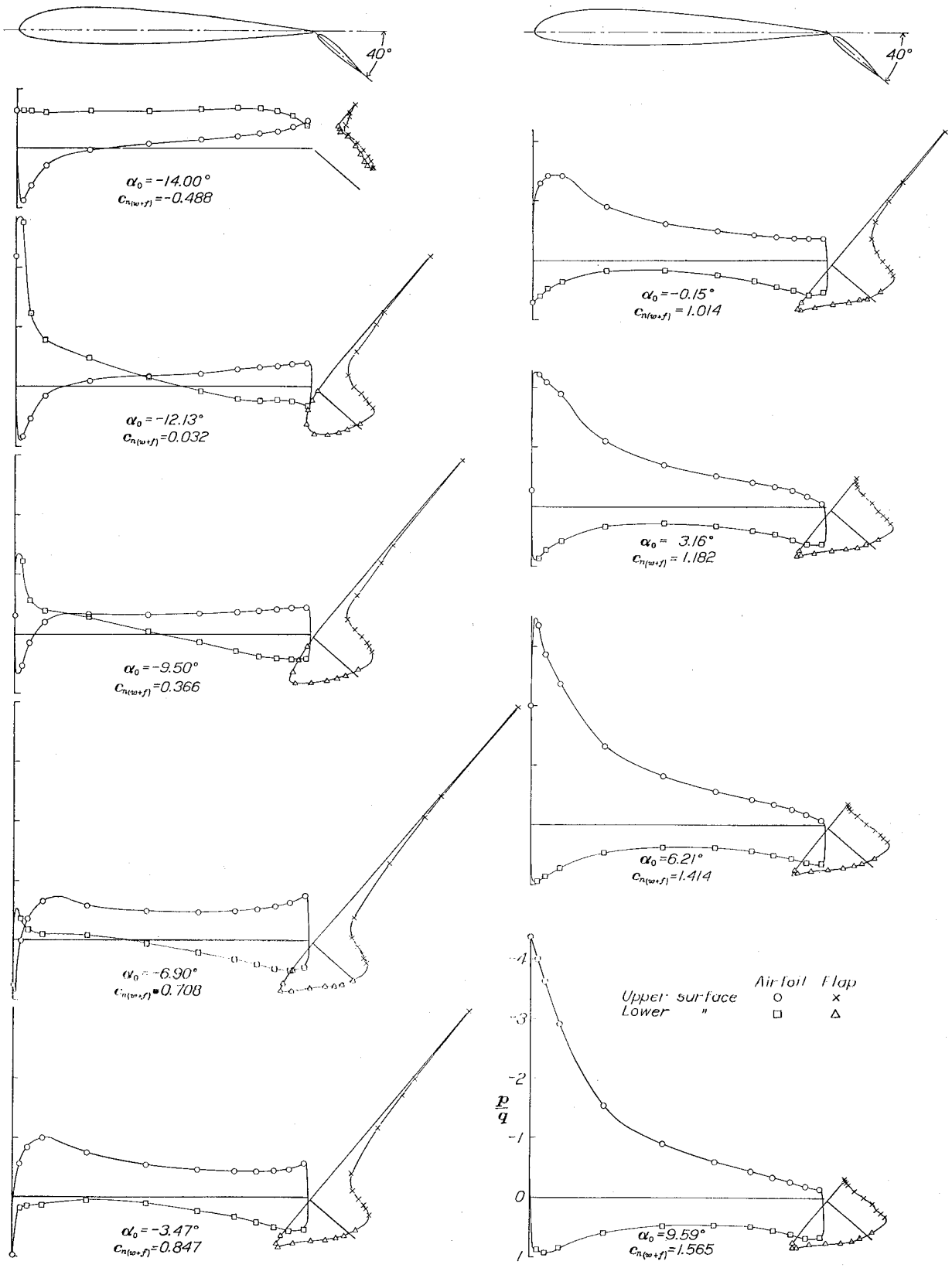

FIGURE 9.—Pressure distribution on the N. A. C. A. 23012 airfoil with N. A. C. A. 23012 external-airfoil flap at various angles of attack. Flap deflected 40°.

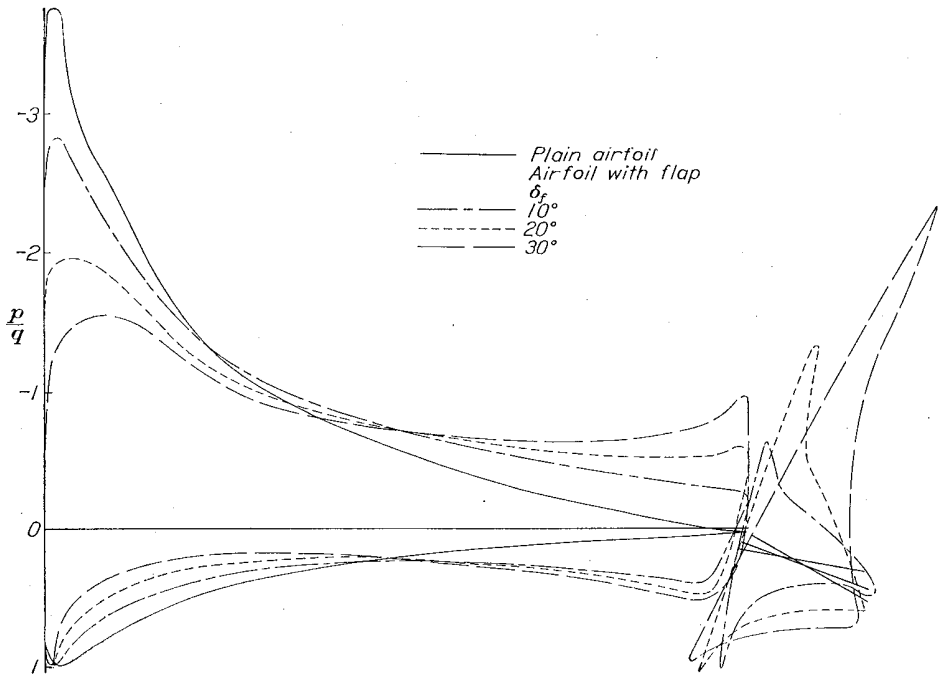

FIGURE 10.—Comparison of the pressure distribution on an N. A. C. A. 23012 airfoil with a $0.20c_w$ external-airfoil flap with that on the plain airfoil at the same lift, $c_n=1.165$.

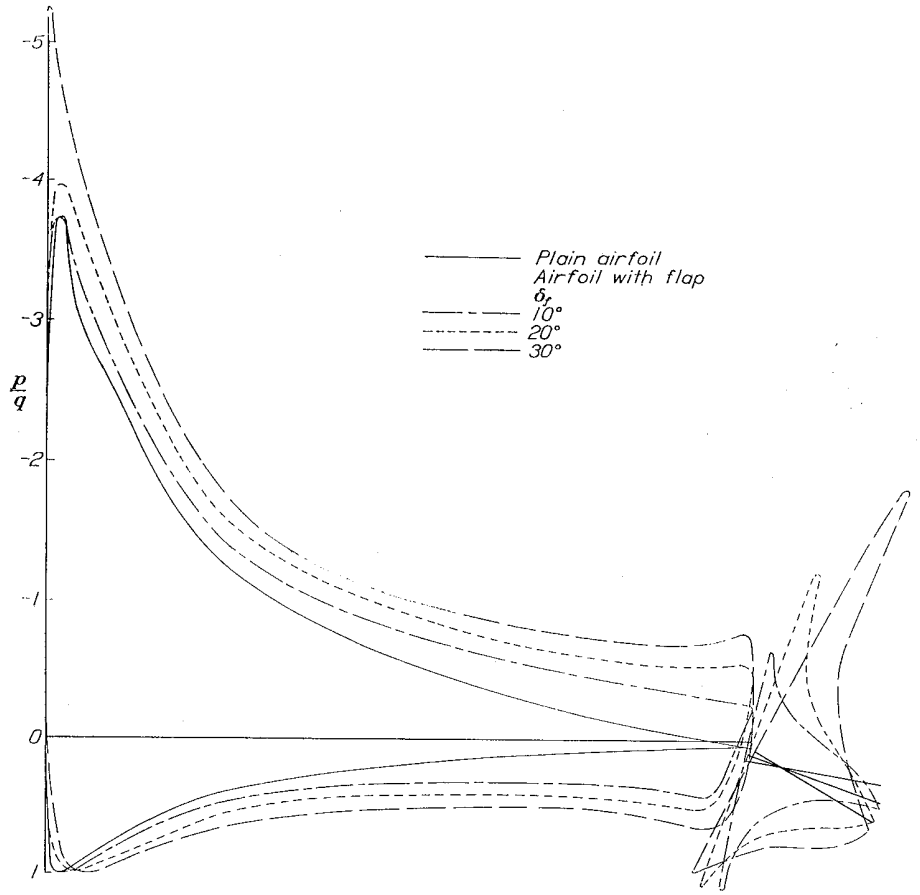

FIGURE 11.—Comparison of the pressure distribution on an N. A. C. A. 23012 airfoil with a $0.20c_w$ external-airfoil flap with that on the plain airfoil at the same angle of attack, $\alpha_0=8.5°$.

COEFFICIENTS

The pressure diagrams were mechanically integrated to obtain data from which section coefficients could be computed. The section coefficients are defined as follows:

$c_{n_w}=\frac{n_w}{qc_w}$, normal-force coefficient of main airfoil alone.

$c_{n_{(w+f)}}=\frac{n_{(w+f)}}{qc_{(w+f)}}$, normal-force coefficient of main airfoil with flap.

$c_{m_w}=\frac{m_w}{qc_w{}^2}$, pitching-moment coefficient of main airfoil alone about quarter-chord point.

$c_{m_{(w+f)}}=\frac{m_{(w+f)}}{qc_{(w+f)}{}^2}$, pitching-moment coefficient of main airfoil with flap about quarter-chord point of combination.

$c_{n_f}=\frac{n_f}{qc_f}$, normal-force coefficient of flap.

$c_{h_f}=\frac{h_f}{qc_f{}^2}$, hinge-moment coefficient of flap about hinge axis.

$(c.\ p.)_w=\left(0.25-\frac{c_{m_w}}{c_{n_w}}\right)\times 100$, center of pressure of main airfoil alone in percentage of chord from leading edge.

$(c.\ p.)_{(w+f)}=\left(0.25-\frac{c_{m_{(w+f)}}}{c_{n_{(w+f)}}}\right)\times 100$, center of pressure of main airfoil with flap in percentage of chord of combination from leading edge.

$(c.\ p.)_f=\left(0.25-\frac{c_{h_f}}{c_{n_f}}\right)\times 100$, center of pressure of flap in percentage of flap chord from leading edge.

where the forces and moments per unit span are

n_w, normal force of main airfoil.

$n_{(w+f)}$, normal force of main airfoil with flap.

m_w, pitching moment of main airfoil about quarter-chord point.

$m_{(w+f)}$, pitching moment of main airfoil with flap about quarter-chord point of combination.

n_f, normal force of flap.

h_f, hinge moment of flap about hinge axis.

and

q, dynamic pressure.

c_w, main-airfoil chord.

c_f, flap chord.

$c_{(w+f)}$ chord of combination (c_w+c_f).

The center-of-pressure positions and the pitching-moment coefficients were derived from the normal forces, the chord forces being neglected except for the effect of the flap, in which case the flap deflection was taken into account.

The calculated results from the present tests were all corrected to infinite aspect ratio characteristics in accordance with methods given by Glauert (reference 6) that have been found satisfactory from other tests of a similar arrangement in the 7- by 10-foot wind tunnel (reference 7). Another check on the theoretical correction is shown in figure 12, where the corrected results of the pressure-distribution tests are compared with force-test results (reference 8) for a 10- by 60-inch N. A. C. A. 23012 plain wing corrected to infinite aspect ratio by the usual methods.

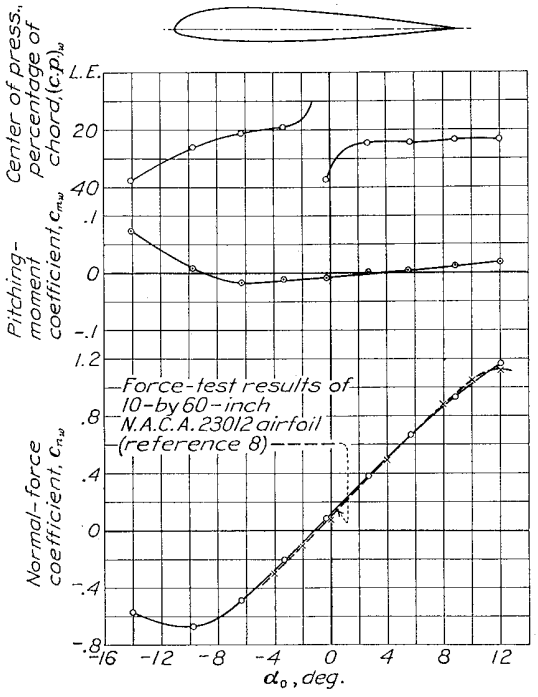

FIGURE 12.—Section characteristics of the plain N. A. C. A. 23012 airfoil.

For the case of the pressure-distribution tests

$$\alpha_0=\alpha+\Delta\alpha$$

where

$$\Delta\alpha(\text{deg.})=-\left(0.25\frac{c}{h}c_n\right)\times 57.3$$

c is the total chord.

h, the height of the jet.

(The quantity c_n is substituted for C_L in the present correction and the substitution results in only a slight error because of the small difference in value between the two quantities.) Curves of the various calculated coefficients are given in figures 12 to 18.

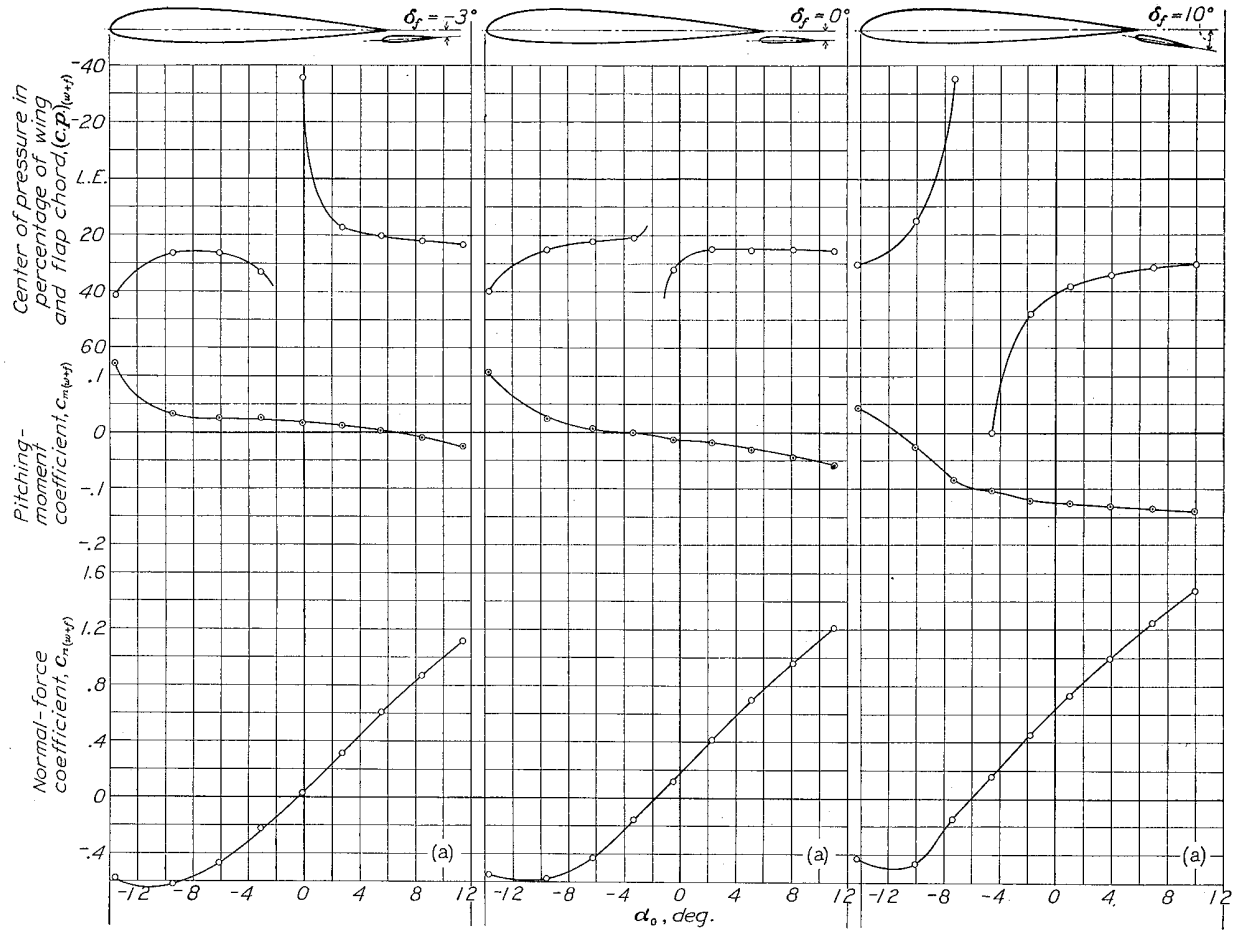

(a) Airfoil with flap.

(a) Airfoil with flap.

(a) Airfoil with flap.

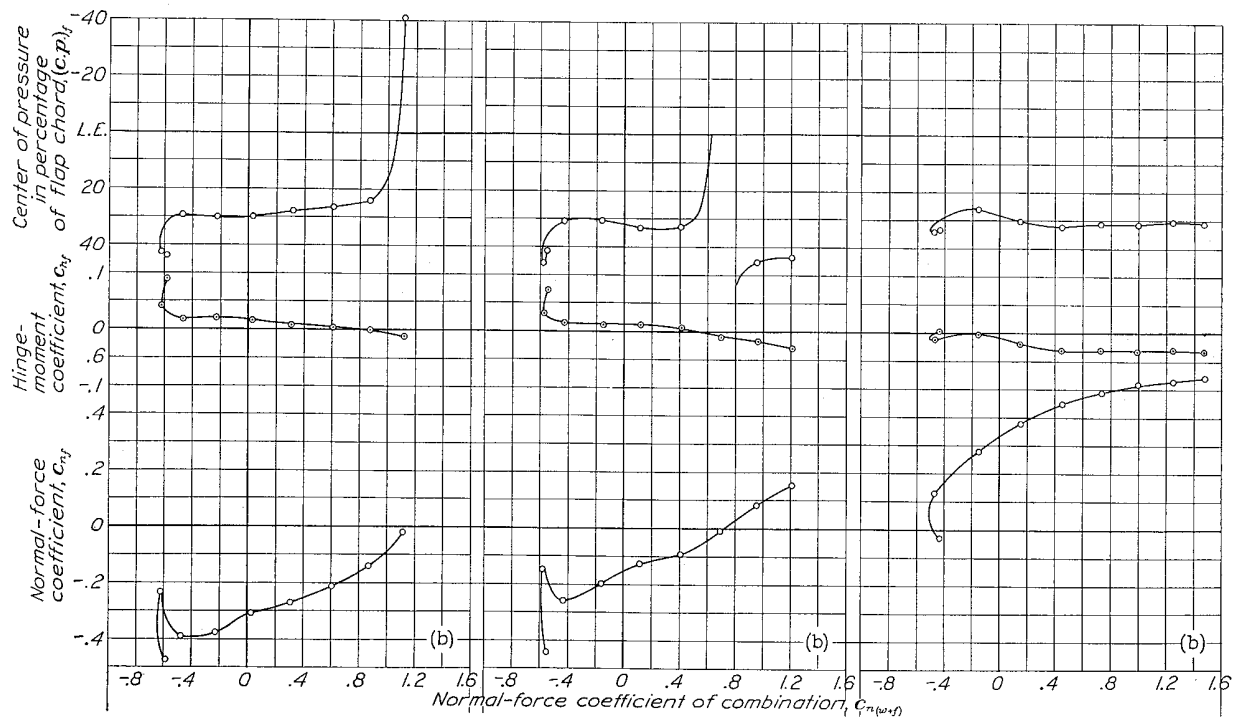

(b) Flap alone.

FIGURE 13.—Section characteristics of the N. A. C. A. 23012 airfoil with a $0.20c_w$ N. A. C. A. 23012 external-airfoil flap set at −3°.

(b) Flap alone.

FIGURE 14.—Section characteristics of the N. A. C. A. 23012 airfoil with a $0.20c_w$ N. A. C. A. 23012 external-airfoil flap set at 0°.

(b) Flap alone.

FIGURE 15.—Section characteristics of the N. A. C. A. 23012 airfoil with a $0.20c_w$ N. A. C. A. 23012 external-airfoil flap set at 10°.

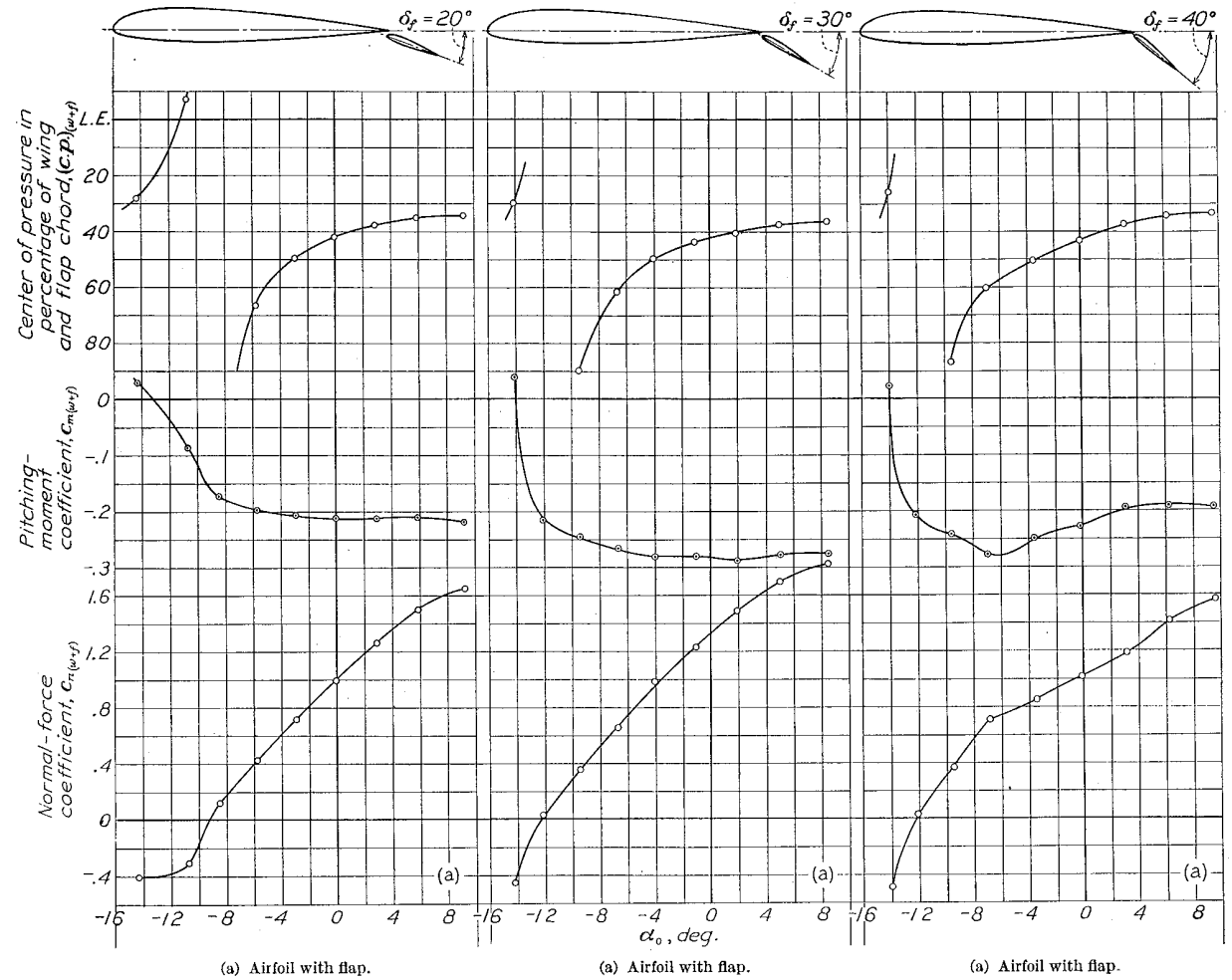

(a) Airfoil with flap.

(a) Airfoil with flap.

(a) Airfoil with flap.

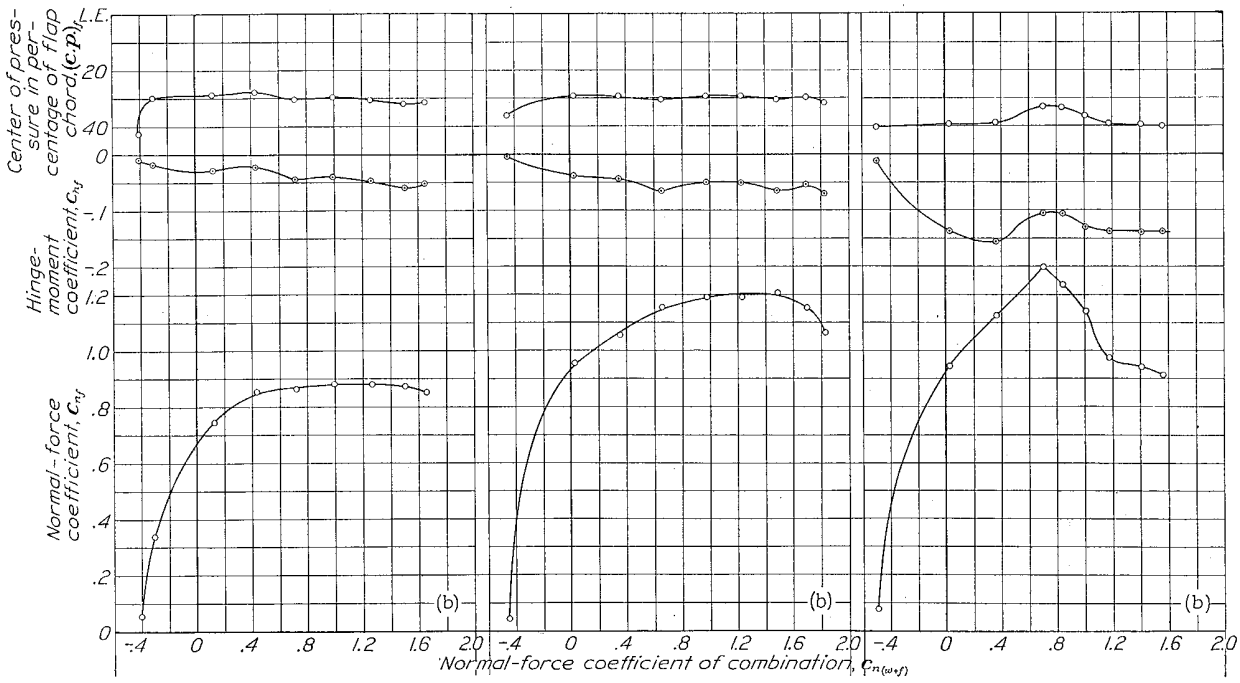

(b) Flap alone.

FIGURE 16.—Section characteristics of the N. A. C. A. 23012 airfoil with a $0.20c_w$ N. A. C. A. 23012 external-airfoil flap set at 20°.

(b) Flap alone.

FIGURE 17.—Section characteristics of the N. A. C. A. 23012 airfoil with a $0.20c_w$ N. A. C. A. 23012 external-airfoil flap set at 30°.

(b) Flap alone.

FIGURE 18.—Section characteristics of the N. A. C. A. 23012 airfoil with a $0.20c_w$ N. A. C. A. 23012 external airfoil flap set at 40°.

PRECISION

No air-flow alinement tests were made in the wind tunnel with the test arrangement used in the investigation, so the absolute setting of the angle of attack may be slightly in error; the relative angles are, however, accurate to $\pm 0.1°$. The flap deflections were set to the specified angles to within $\pm 0.1°$. The orifice pressures based on check tests in which both the angle of attack and the flap settings were independently changed showed that they agreed to within ± 2 percent, with the exception of upper-surface pressures near the leading edges, which, at high angles of attack, checked to within ± 5 percent. The dynamic pressure recorded on each diagram was accurate to within ± 0.25 percent for all tests.

The distribution of pressures along the span of the model indicated that two-dimensional flow was obtained with the installation used. The pressures, for a given location along the chord of the airfoil, were the same from midspan to within at least ½ inch of the ends (the row of orifices nearest the end of the model).

RESULTS AND DISCUSSION

SECTION PRESSURE DISTRIBUTION

The pressure-distribution diagrams (figs. 3 to 9) are useful to show the chordwise distribution of the air loads on the main airfoil and on the flap and may be regarded as satisfactory for application to rib and flap design. The diagrams also illustrate certain special features of the action of external-airfoil flaps.

Comparison of pressure diagrams for the plain airfoil and for the airfoil-flap combination at the *same lift* (fig. 10) shows the effect of the flap. Increasing the flap angle and decreasing the angle of attack to maintain constant lift had the following effects: (1) The magnitudes of the peak pressures at the leading edge of the main airfoil were progressively reduced, and (2) the magnitudes of both positive and negative pressures at the trailing edge of the main airfoil and at the leading edge of the flap were progressively increased.

The flap, in addition, obstructed the flow of air below the airfoil and caused the pressures to build up on the lower surface. The air flowing through the slot over the upper surface of the flap produced a higher average velocity and increased the negative pressure on the flap upper surface. Thus, the influence of the flap was to reduce the adverse pressure gradients and the tendency of the main airfoil to stall.

The external-airfoil flap itself had a pressure distribution similar to that of a plain airfoil, so that the flap would have a small wake as long as it remained unstalled. The wake of the combination would therefore be small, particularly near the stall; this small wake permitted the development of high lift together with low profile drag. In this respect slotted flaps, in general, appear better than plain or split flaps.

Comparison of pressure diagrams for the plain airfoil and for the airfoil-flap combination at the *same angle of attack* (fig. 11) shows that the flap increased the negative pressure over the entire upper surface of the main airfoil and increased the positive pressure on the lower surface near the trailing edge. The pressure gradients remained about the same except at the trailing edge of the main airfoil, where they were reduced. The pressures on the upper and the lower surfaces of the flap both increased with flap deflection. The important effect of the flap in this case was its ability to influence the air flow around the main airfoil so that the airfoil carried a much greater load without stalling than was possible without the flap.

One other interesting item is suggested by the progressive increase in flow velocity over the main-airfoil upper surface relative to free-stream velocity as the flap is deflected. This characteristic suggested that the use of this type of flap would increase the rolling effectiveness of ailerons located on the trailing edge of the main airfoil. An investigation of such an arrangement (reference 3) recently completed in the N. A. C. A. 7- by 10-foot wind tunnel indicated that such an improvement could be realized.

SECTION LOADS AND MOMENTS

The section coefficients are plotted in figures 12 to 18. It will be noted that the flap loads build up rapidly at relatively low lifts of the combination and that they also increase rapidly with flap deflection (figs. 13 to 18). The maximum flap loads appear, in general, to reach somewhat higher values than are obtained with an airfoil of the same size tested alone at the appropriate Reynolds Number. (Test Reynolds Number for flap alone based on flap chord and free-stream velocity= 244,000.) The greater part of the increment of total $c_{n_{max}}$ due to deflecting the flap downward, however, arises from the increased load carried by the main airfoil.

It is interesting to note that the maximum normal-force coefficient of the external-airfoil flap tested has about the same value as that attained by split flaps in a previous investigation (reference 9). Owing to the use of the hinge axis chosen, however, the hinge moments of the external-airfoil flap are much smaller than those of corresponding sizes of split flap.

CONCLUSIONS

1. Pressure-distribution tests show that, as with other types of flap, the greater part of the increment of total maximum lift due to deflecting the external-airfoil flap downward arises from the increased load carried by the main airfoil.

2. The maximum normal-force coefficient of the external-airfoil flap investigated had about the same value as that attained by split flaps. The hinge mo-

ments, however, were much lower because of the axis location used with the external-airfoil flap.

3. The pressure diagrams showed that, when the plain airfoil and the airfoil with the external-airfoil flap were compared at the *same total lift*, the flap reduced the adverse pressure gradients and the tendency of the main airfoil to stall. When these plain and flapped airfoils were compared at the *same angle of attack*, it was apparent that the flap influenced the air flow around the main airfoil so that the airfoil carried a much greater load without stalling than was possible without the flap.

LANGLEY MEMORIAL AERONAUTICAL LABORATORY,
NATIONAL ADVISORY COMMITTEE FOR AERONAUTICS,
LANGLEY FIELD, VA., *July 29, 1937.*

REFERENCES

1. Platt, Robert C.: Aerodynamic Characteristics of Wings with Cambered External-Airfoil Flaps, Including Lateral Control with a Full-Span Flap. T. R. No. 541, N. A. C. A., 1935.
2. Platt, Robert C., and Abbott, Ira H.: Aerodynamic Characteristics of N. A. C. A. 23012 and 23021 Airfoils with 20-Percent-Chord External-Airfoil Flaps of N. A. C. A. 23012 Section. T. R. No. 573, N. A. C. A., 1936.
3. Platt, Robert C., and Shortal, Joseph A.: Wind-Tunnel Investigation of Wings with Ordinary Ailerons and Full-Span External-Airfoil Flaps. T. R. No. 603, N. A. C. A., 1937.
4. Harris, Thomas A.: The 7 by 10 Foot Wind Tunnel of the National Advisory Committee for Aeronautics. T. R. No. 412, N. A. C. A., 1931.
5. Platt, Robert C.: Turbulence Factors of N. A. C. A. Wind Tunnels as Determined by Sphere Tests. T. R. No. 558, N. A. C. A., 1936.
6. Glauert, H.: Wind Tunnel Interference on Wings, Bodies, and Airscrews. R. & M. No. 1566, British A. R. C., 1933.
7. Wenzinger, Carl J.: Wind-Tunnel Investigation of the Aerodynamic Balancing of Upper-Surface Ailerons and Split Flaps. T. R. No. 549, N. A. C. A., 1935.
8. Wenzinger, Carl J.: Wind-Tunnel Investigation of Ordinary and Split Flaps on Airfoils of Different Profile. T. R. No. 554, N. A. C. A., 1936.
9. Wenzinger, Carl J.: Wind-Tunnel Measurements of Air Loads on Split Flaps. T. N. No. 498, N. A. C. A., 1934.

U. S. GOVERNMENT PRINTING OFFICE: 1937

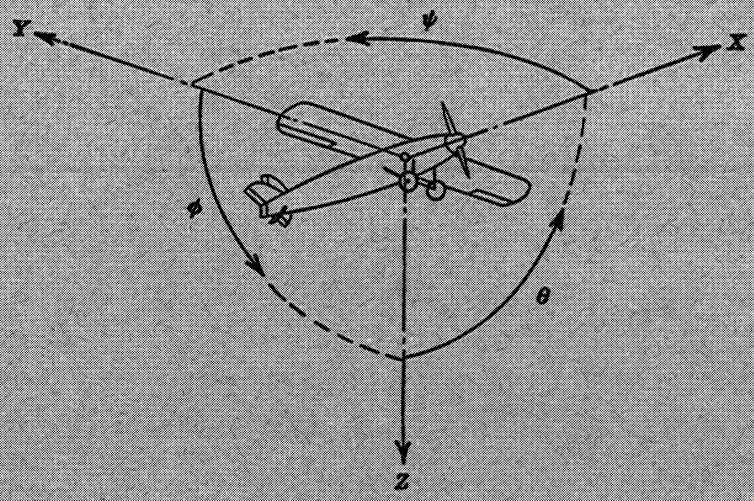

Positive directions of axes and angles (forces and moments) are shown by arrows

Axis		Force (parallel to axis) symbol	Moment about axis			Angle		Velocities	
Designation	Symbol		Designation	Symbol	Positive direction	Designation	Symbol	Linear (component along axis)	Angular
Longitudinal	X	X	Rolling	L	$Y \longrightarrow Z$	Roll	ϕ	u	p
Lateral	Y	Y	Pitching	M	$Z \longrightarrow X$	Pitch	θ	v	q
Normal	Z	Z	Yawing	N	$X \longrightarrow Y$	Yaw	ψ	w	r

Absolute coefficients of moment

$C_l = \frac{L}{qbS}$ (rolling) $\quad C_m = \frac{M}{qcS}$ (pitching) $\quad C_n = \frac{N}{qbS}$ (yawing)

Angle of set of control surface (relative to neutral position), δ. (Indicate surface by proper subscript.)

4. PROPELLER SYMBOLS

D, Diameter

p, Geometric pitch

p/D, Pitch ratio

V', Inflow velocity

V_s, Slipstream velocity

T, Thrust, absolute coefficient $C_T = \frac{T}{\rho n^2 D^4}$

Q, Torque, absolute coefficient $C_Q = \frac{Q}{\rho n^2 D^5}$

P, Power, absolute coefficient $C_P = \frac{P}{\rho n^3 D^5}$

C_s, Speed-power coefficient $= \sqrt[5]{\frac{\rho V^5}{P n^2}}$

η, Efficiency

n, Revolutions per second, r.p.s.

Φ, Effective helix angle $= \tan^{-1}\left(\frac{V}{2\pi r n}\right)$

5. NUMERICAL RELATIONS

1 hp. = 76.04 kg-m/s = 550 ft-lb./sec.
1 metric horsepower = 1.0132 hp.
1 m.p.h. = 0.4470 m.p.s.
1 m.p.s. = 2.2369 m.p.h.

1 lb. = 0.4536 kg.
1 kg = 2.2046 lb.
1 mi. = 1,609.35 m = 5,280 ft.
1 m = 3.2808 ft.